

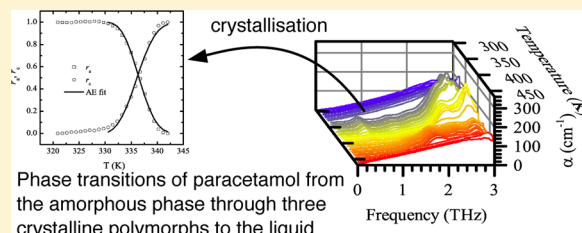
# Crystallization and Phase Changes in Paracetamol from the Amorphous Solid to the Liquid Phase

Juraj Sibik, Michael J. Sargent, Miriam Franklin, and J. Axel Zeitler\*

Department of Chemical Engineering and Biotechnology, University of Cambridge, New Museums Site, Pembroke Street, Cambridge CB2 3RA, United Kingdom

**ABSTRACT:** For the case of paracetamol, we show how terahertz time-domain spectroscopy can be used to characterize the solid and liquid phase dynamics. Heating of supercooled amorphous paracetamol from 295 K in a covered sample under vacuum leads to its crystallization at 330 K. First, form III is formed followed by the transformation of form III to form II at 375 K, to form I at 405 K, and finally melting is observed around 455 K. We discuss the difference between the featureless spectra of the supercooled liquid and its liquid melt. Lastly, we studied the onset of crystallization from the supercooled liquid in detail and quantified its kinetics based on the Avrami–Erofeev model. We determined an effective rate constant of  $k = 0.056 \text{ min}^{-1}$  with a corresponding onset of crystallization at  $T = 329.5 \text{ K}$  for a heating rate of  $0.4 \text{ K min}^{-1}$ .

**KEYWORDS:** terahertz spectroscopy, paracetamol, acetaminophen, amorphous, crystallization, polymorph, kinetics



## INTRODUCTION

For drug delivery by solid oral dosage forms, the formulation contains an active pharmaceutical ingredient (API) either in one of its crystalline or in an amorphous form. Although given its lower energy state and better long-term stability properties, where typically the crystalline form is preferred, amorphous API formulations are of intense interest due to their higher intrinsic solubility.<sup>1</sup> Formulation of amorphous drugs may, however, lead to an undesired crystallization during the shelf life of the dosage form.<sup>2,3</sup> It is therefore crucial to understand and control the mechanisms involved in the crystallization from the amorphous phase.

Paracetamol is a common analgesic drug, widely used as a painkiller and for its antipyretic effects. Three crystalline forms have been reported to date. These can be arranged from the most stable at standard temperature and pressure as form I > form II > form III.<sup>4</sup> It is also relatively straightforward to supercool the melt and prepare an amorphous form, which is the least stable of all its solid forms.<sup>5,6</sup> Despite its well-characterized solid forms, paracetamol exhibits a peculiar crystallization behavior that is strongly affected by minor experimental conditions.<sup>7,8</sup> A recent study by Nanubolu et al. has offered a comprehensive comparison between various experimental conditions and crystallization patterns.<sup>9</sup> It has been found that, while the uncovered samples are predominated by surface crystallization into forms I and II, the covered samples are dominated by bulk crystallization into form III.

The characterization of amorphous materials is complicated by the lack of well-defined structure and the strong dependence on the thermal history which is common to all amorphous materials. Structural solid-state characterization techniques such as X-ray diffraction (XRD) cannot easily differentiate between amorphous solids that differ energetically. The thermal history

has a strong effect on the thermodynamic properties of the glasses, which in turn are easier to quantify: thermo-analytical techniques such as (modulated) differential scanning calorimetry (DSC) and thermally stimulated depolarization current measurements<sup>10,11</sup> offer a straightforward way to determine the glass transition temperature, the onset of the molecular mobility and crystallization. In order to create a more comprehensive microscopical image it is however necessary to use spectroscopic and scattering techniques.<sup>12</sup> One commonly used technique that is used for such characterization is dielectric spectroscopy, which can cover an extremely broad range of frequencies from  $10^{-3} \text{ Hz}$  up to  $10^9 \text{ Hz}$ , and possibly up to  $10^{12} \text{ Hz}$  when quasi-optical techniques are involved. The dielectric spectra in this frequency range reveal primary and secondary relaxation processes in the supercooled liquids and glasses. Several studies suggested that the (primary) relaxation time may be used for an estimation of the amorphous pharmaceutical stability during storage.<sup>13,14</sup> Later studies however emphasized the importance for including the localized motions of the Johari–Goldstein secondary relaxation in the predictions<sup>6,15,16</sup> and the caveat that these estimations are not universally valid.<sup>17</sup> In addition, inelastic incoherent neutron scattering studies revealed that the fast secondary relaxations occurring at nanosecond time scales play a crucial role in the protein stabilization in glasses.<sup>18,19</sup>

A relatively novel technique for the characterization of solid-state pharmaceuticals is terahertz time-domain spectroscopy (THz-TDS, typically covering frequencies between 0.1 and 4

**Received:** December 20, 2013

**Revised:** February 25, 2014

**Accepted:** February 28, 2014

**Published:** February 28, 2014

THz).<sup>20,21</sup> The strength of terahertz spectroscopy lies in its ability to probe the intermolecular excitations in materials that are too fast to measure with dielectric spectroscopy yet at too low energies for far-infrared spectroscopy. THz-TDS has several additional practical advantages, such as being a nondestructive, nonionizing, contact-free, phase-sensitive technique, and experiments are performed using average power levels on the order of microwatts with no danger of inducing any structural modification due to the experimental radiation.<sup>22</sup> Organic molecular crystals usually exhibit distinct spectral fingerprints at terahertz frequencies that can be exploited to identify polymorphic forms,<sup>23,24</sup> hydrates,<sup>25</sup> or cocrystals,<sup>26,27</sup> often with sensitivities exceeding that of other vibrational spectroscopy techniques due to the fact that vibrational modes at terahertz frequencies originate from the intermolecular interactions within the crystal structure rather than from intramolecular modes, which dominate the spectra at higher frequencies.

Terahertz spectroscopy is emerging also as a useful complementary characterization tool in the field of disordered materials.<sup>28,29</sup> It was shown that all terahertz spectra of disordered materials are featureless due to a universal coupling mechanism of terahertz radiation into the vibrational density of states (VDOS).<sup>30</sup> Terahertz spectroscopy was used to study atomic charge distributions of sodosilicate glasses,<sup>31</sup> optical properties in a very broad frequency range of 0.2–18 THz of chalcogenide glasses,<sup>32</sup> and the glass transition in polymers.<sup>33,34</sup> A recent study of aqueous sorbitol solutions showed that the absorption originating from the VDOS becomes gradually dominated by the dielectric relaxation processes as the molecular glasses are heated above their respective glass transition temperature.<sup>35,36</sup> Given the fundamental difference between the spectra of disordered and ordered systems, terahertz spectroscopy is ideally suited to monitor the crystallization of amorphous drugs<sup>37</sup> or polymers<sup>38</sup> and distinguish between different solid-state modifications.

In the present study, we aim to extend the current state of understanding using terahertz spectroscopy of the amorphous phase and its crystallization. With the example of paracetamol, we show the wealth of information that can be extracted from the terahertz spectra of a supercooled liquid and liquid melt, which might at first sight be erroneously mistaken to be rather boring due to their featureless nature. We show that the mechanism and level of absorption at terahertz frequencies is different in such phases and that this behavior can be extracted from the spectra using a simple power law model. Lastly, we show how this information can be used to determine the onset of crystallization in supercooled liquids.

## METHODS

**Materials.** Paracetamol (acetaminophen, 99% purity) was obtained from Sigma-Aldrich, UK. Polyethylene powder (particle size <10  $\mu\text{m}$ ) was obtained from Induchem, Volketswil, Switzerland. Materials were used without further processing.

**Crystalline Sample Preparation.** For the room temperature THz-TDS measurements, 60 mg of crystalline paracetamol was mixed with 300 mg of polyethylene powder, loaded, and compressed into a pellet using a hydraulic pellet press at a force of 2 tons. For the reference, a pellet made of 300 mg of polyethylene powder was used.

**Amorphous Sample Preparation.** A sample of crystalline paracetamol was heated to  $\sim 460$  K (187 °C) on a hot plate until fully melted. In order to eliminate degradation, it was

ensured that the melt remains as a clear liquid and does not turn yellow to any visible extent. The sample holder was a sandwich structure consisting of two circular crystalline z-cut quartz windows (1.5 mm thickness, 13 mm diameter) separated by a spacer made from mylar with a nominal thickness of 190  $\mu\text{m}$ . The spacer had an aperture of 9 mm in diameter in its center that was fully filled with the melt of paracetamol. The sandwich structure was then placed into a metal holder that was screwed to a copper block with an aperture of 9 mm, sealing the melt between the two windows (Figure 1). At this point, the sample was removed from the hot plate and cooled to room temperature (295 K) by placing the copper block on a large metal table.

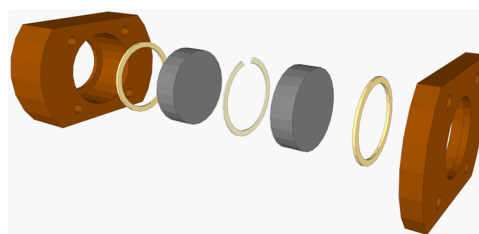


**Figure 1.** Quartz window sample holder. The quartz windows are pressed together by a copper cradle, with PTFE rings between the quartz and copper to allow for differential thermal expansion. The sample is held in the mylar spacer between the windows, with a slit cut in it. This cradle is then bolted to the coldfinger of the cryostat.

**Variable Temperature THz-TDS.** Following amorphous sample preparation, the copper block was attached to the coldfinger of a cryostat (modified continuous flow ST-100 FTIR, Janis, Wilmington, MA, USA) and mounted in the vacuum chamber of a THz-TDS setup. For the reference measurements, we used two 1.5 mm thick quartz windows with no spacer between that were mounted just below the sample onto the same copper coldfinger of the cryostat.

The sample was heated from 295 to 470 K in 5 K steps under vacuum. Upon reaching each temperature increment, the system was allowed to equilibrate for 5 min. After this time, the reference measurement was acquired in transmission geometry as described elsewhere,<sup>39</sup> followed by the sample measurement. Each measurement took 4 min by co-averaging 200 time-domain waveforms. Overall, the sample was equilibrated for approximately 10 min prior to the acquisition of the respective terahertz spectrum. The optical properties of the sample were extracted in the frequency range of 0.1–3.0 THz using fast Fourier transformation of the time-domain waveforms.

For the detailed study of the crystallization kinetics of paracetamol from its amorphous form, a sample was prepared in the same way as described in the sample preparation section above. The sample was then heated from room temperature to 320 K in 5 K steps, and spectra were acquired in order to confirm that no crystallization had yet taken place over this temperature range. The sample was then heated continuously from 320 to 340 K with a heating rate of 0.4 K  $\text{min}^{-1}$ . Terahertz spectra of the sample were acquired at a scan rate of 1 Hz throughout this period. In order to increase the signal-to-noise ratio of the resulting spectra, 120 time-domain waveforms were averaged for each data point, resulting in an effective temperature resolution of 0.8 K.

**Terahertz Power Law Model.** It was previously shown that the absorption of glasses at terahertz frequencies can be well-described by a combination of  $\sim\omega^2$  and  $\sim\omega^4$  power laws that may be ascribed to uncorrelated (due to long-range disorder) and correlated (due to local charge neutrality) charge fluctuations, respectively.<sup>30</sup> The uncorrelated part of the absorption usually dominates,<sup>31</sup> and therefore, one power law with an exponent close to 2 is usually a good fit of the data, as shown originally by Strom.<sup>40</sup>

We recently demonstrated that the terahertz spectra obey the power law not only in the glassy state but also in supercooled liquid as well as liquid phases, as the spectra remain without sharp spectral features.<sup>35</sup> Overall, the absorption coefficient multiplied by the refractive index, that is, the real part of the conductivity, in the nonionic liquids may be described by<sup>35</sup>

$$n(\nu)\alpha(\nu) = A + C(\nu - \nu_0)^q \quad (1)$$

where  $\nu$  is frequency and  $C$  describes the strength of the coupling of terahertz radiation to the amorphous matter. As outlined above, the exponent  $q$  is close to 2 in the glassy state where losses are dominated by the VDOS and decreases toward 1 as the sample is heated above the glass transition temperature,  $T_g$ , where losses become dominated by the dielectric relaxation. The parameters  $A$  and  $\nu_0$  were introduced to account for the fact that the experimental terahertz spectra are acquired only from some positive frequency  $\nu_0$  (here 0.1 THz), and the absorption at this frequency may be nonzero. Thus  $A$  represents absorption at  $\nu_0$  and is strongly related to the tail of the dielectric relaxation processes occurring at lower frequencies.<sup>35</sup>

**Differential Scanning Calorimetry (DSC).** The crystallization and melting dynamics were further evaluated with DSC. Two scans were performed. The first scan was used to determine the actual polymorph of the crystalline paracetamol measured by THz-TDS at room temperature. Five milligrams of crystalline sample was loaded into an aluminum pan and crimped (closed with a lid). The calorimetric measurement was performed with a TA Instruments Q2000 calorimeter from room temperature to 470 K at 10 K  $\text{min}^{-1}$ .

The second scan was used to accurately determine the onset of crystallization in amorphous paracetamol. For this purpose, 5 mg of crystalline sample was loaded into an aluminum pan and crimped. The sample was then heated to 453 K, melted, quenched down to 298 K, heated to 320 K, equilibrated for 15 min, and measured from 323 to 373 K at a rate of 0.4 K  $\text{min}^{-1}$ , which matches the heating rate of the variable temperature THz-TDS experiment described above.

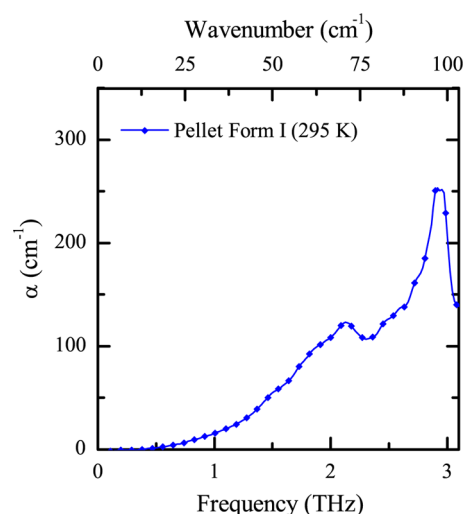
## RESULTS

### DSC and Terahertz Analysis of Paracetamol Form I.

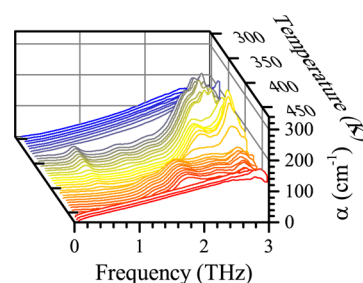
DSC measurements revealed a melting endotherm at 442 K (169 °C), indicative of paracetamol form I, the most stable polymorph at room temperature.<sup>9</sup> The thermal analysis revealed no other thermal events, indicating that only form I was present.

The terahertz spectra of the paracetamol pellet obtained at room temperature are shown in Figure 2. The spectra reveal two vibrational modes at around 2.1 and 3.0 THz. A weak shoulder is also resolved at around 1.5 THz.

**Variable Temperature THz-TDS.** The absorption terahertz spectra over the full temperature range of 295–470 K are shown in Figure 3. The absorption coefficient at several chosen frequencies is shown as a function of temperature in



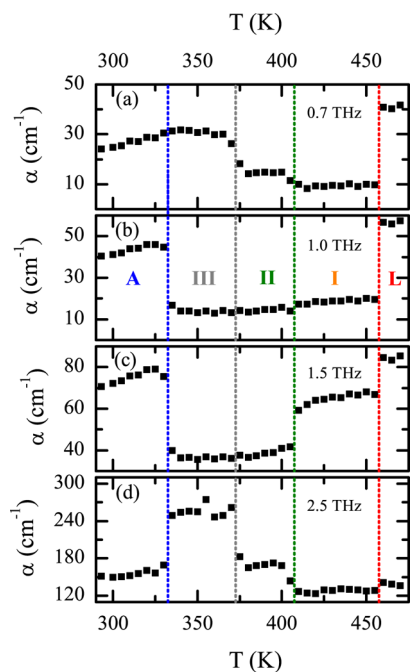
**Figure 2.** Absorption spectrum extracted from the sample pellet composed of crystalline paracetamol form I at 295 K.



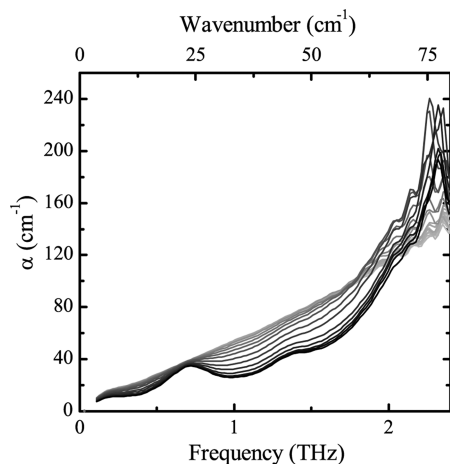
**Figure 3.** Absorption spectra of paracetamol at terahertz frequencies upon heating the sample from the supercooled liquid phase over the temperature range of 295–470 K in 5 K increments.

Figure 4. The lowest temperature at which we acquired spectra, 295 K, is very close to the glass transition temperature of paracetamol,  $T_g = 296$  K. At the lowest temperatures, the sample is therefore considered to be in the supercooled liquid state. The absorption of the supercooled liquid increases monotonously with frequency and temperature, and no spectral features can be observed. At about  $335 \pm 5$  K, crystallization occurs from the supercooled liquid, which results in a dramatic change in the terahertz spectra, and two peaks, one at 0.7 THz and the other at around 2.5 THz, emerge. As the sample is heated further, the spectral features change at around  $375 \pm 5$  K and again at  $405 \pm 5$  K, signaling two solid–solid transitions between different polymorphs of crystalline paracetamol (Figure 3). The sample finally melts at around  $455 \pm 5$  K. The spectral features disappear again, and once again, the spectra are dominated by a monotonous increase in absorption with frequency, similar in shape and magnitude to what was previously observed for the spectra of the supercooled liquid.

**Detailed Study of Crystallization.** The absorption terahertz spectra obtained during the detailed investigation of the onset of crystallization using the continuous heating method in the temperature range of 320–340 K are shown in Figure 5. At temperatures below 330 K (light gray), the sample stayed amorphous, slightly increasing in absorption with temperature. As the sample was heated above 330 K, the spectra with narrow spectral features around 0.7, 1.4, and 2.5 THz began to emerge from the monotonous background, which is a clear signature of crystallization of paracetamol.



**Figure 4.** Absorption coefficient of paracetamol at (a) 0.7 THz, (b) 1.0 THz, (c) 1.5 THz, and (d) 2.5 THz in the temperature range of 295–470 K with 5 K increments. The vertical dotted lines separate different states of paracetamol: A = amorphous, III, II, I = crystalline polymorphs, and L = liquid.



**Figure 5.** Absorption spectra of paracetamol at terahertz frequencies upon heating the sample continuously from 320 to 340 K (light gray to dark lines in 0.8 K intervals) at a heating rate of 0.4 K min<sup>-1</sup>.

During the last 2 K of heating, the sample of the spectra ceased to change, indicating a completion of the crystallization process.

## DISCUSSION

**Identification of Crystalline Polymorphs of Paracetamol.** In Figure 6a, we compare the terahertz spectra of all the different crystalline polymorphs that were observed by heating the sample of amorphous paracetamol in this study. The spectral features of an organic molecular crystal at terahertz frequencies typically originate from intermolecular vibrations and librations, given the relatively low energy of the modes, though some additional intramolecular flexibility can also be observed, in particular, for larger molecules.<sup>41–43</sup>

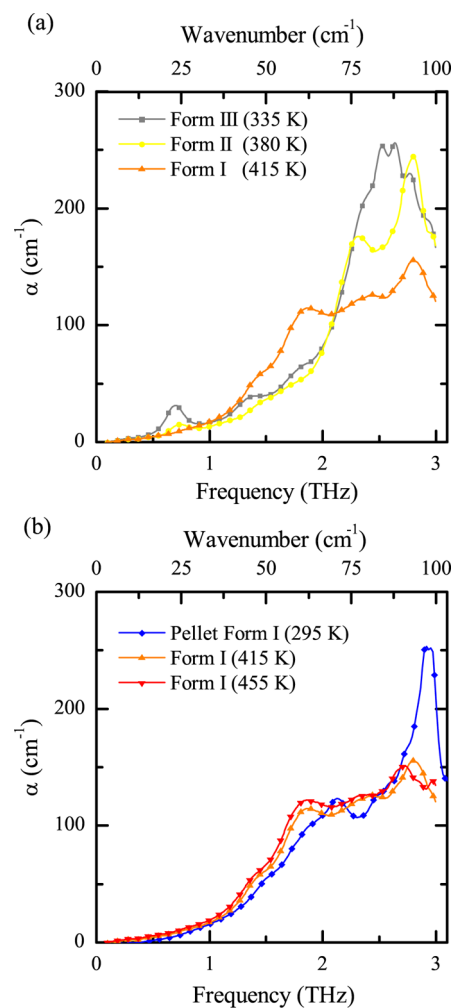


**Figure 6.** (a) Absorption spectra of different crystalline forms of paracetamol; (b) thermal shift of spectral lines of form I between 295 (pellet), 415, and 455 K (crystallized amorphous form).

It is important to keep in mind that the spectra in Figure 6 were acquired in situ over a range of temperatures and that the intermolecular modes will shift in frequency due to the change in temperature. Here, all modes show a red shift upon heating, which is in good agreement with previous studies.<sup>24,44</sup> The extent of the red shift, and associated change in spectral intensity, is highlighted in Figure 6b for form I, where the peak that is observed at around 2.8 THz at room temperature shifts by  $\sim 0.05$  THz to lower frequencies upon heating from 415 to 455 K (i.e., by 40 K). Based on this observation and by using linear extrapolation, it may be thus concluded that at room temperature, 295 K, this mode would sit at around 2.95 THz, which is in good agreement with the peak observed in the terahertz spectra of the pellet of paracetamol form I (Figure 2). The assignment of the spectra between 415 and 455 K to form I is further supported by the complete lack of any feature at around 0.7 THz, which is present in both of the other polymorphs. We conclude that at temperatures just below the melting point paracetamol has crystallized into form I. This is in agreement with the fact that, thermodynamically, form I is the most stable known polymorph.

A recent comprehensive Raman microscopy study of paracetamol showed that different crystallization behavior from the amorphous phase is strongly dependent on the

environmental conditions, that is, whether the sample is covered or uncovered, during crystallization.<sup>9</sup> In the case of a covered sample, which is also the case in this study since the sample is sealed between two quartz windows and the measurement takes place under vacuum, amorphous paracetamol crystallized, in this order, first to form III (323–329 K), followed by two phase transitions to forms II (385–391 K) and I (421 K) upon heating.<sup>9</sup> We observe a crystallization from the amorphous phase at 330 K followed by two phase transitions at 370 and 405 K (Figure 4), and given the proximity in temperature to the crystallization events reported by Nanubolu and Burley (considering the differences in heat transfer and sample size between the Raman and terahertz setups), we conclude that we observe forms III, II, and I as well as melting of form I at around  $455 \pm 5$  K upon heating the sample of amorphous paracetamol.

#### Supercooled Liquid and Liquid Melt of Paracetamol.

Aside from identification of crystalline forms, we recently showed that THz-TDS can be used also to differentiate between distinct regimes of supercooled liquids.<sup>35</sup> Well below  $T_g$ , the terahertz spectra of amorphous solids are well-described by a coupling of the terahertz radiation into the vibrational (and/or librational) density of states, VDOS, as outlined above.

As the amorphous sample is heated toward and above  $T_g$ , dielectric relaxations happen at shorter time scales and shift up in frequency into the terahertz frequency range. This leads to an increase in absorption mainly at the lower end of the spectra that can be measured by THz-TDS. This effect is best illustrated in Figure 7 by plotting the imaginary part of the dielectric losses,  $\epsilon'' = c n \alpha / (2\pi\nu)$ , as this representation is the common practice used in the dielectric spectroscopy literature.

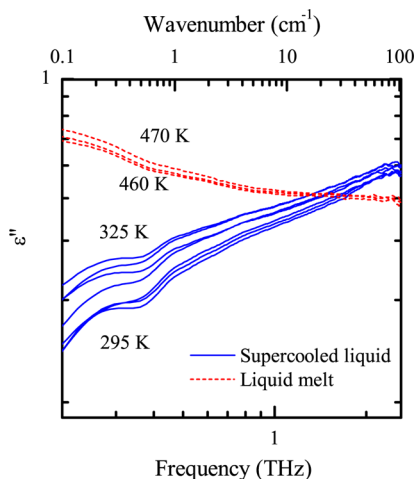


**Figure 7.** Dielectric losses of supercooled liquid paracetamol between 295 and 325 K (blue solid lines) and liquid melt paracetamol between 460 and 470 K (red dashed lines).

At low temperatures, the spectrum is dominated by the low-frequency part of the VDOS peak centered about 2–3 THz (only the low-frequency wing of this peak is accessible using THz-TDS). From Figure 7, it is apparent that the dielectric relaxation processes cause an increase of the losses in the spectrum below 1 THz. This is expected<sup>35</sup> given that the lowest experimental temperature in this experiment is above  $T_g$ . The exact center frequency of the VDOS peak cannot be determined accurately due to the limited spectral window. It is interesting to note that at frequencies above 1.5 THz the

losses measured in the liquid of the melt are lower than the losses of the supercooled liquid. One would expect the magnitude of the losses in the melt to be close to that of supercooled liquid and glasses, that is, at the level of the VDOS. At present, the origin of this difference remains somewhat unclear. Commonly, a decrease in the intensity and a red shift of the excess VDOS over the Debye level is observed upon heating a glass; this however is influenced by a faster increase of the Debye level over the overall VDOS of amorphous material rather than a decrease in overall VDOS.<sup>45</sup> In similar terahertz spectroscopy studies, where a glass was heated to high temperatures, no decrease of losses was observed upon heating at any frequency in the range of 0.1–3 THz.<sup>35,36</sup> In this previous work, the samples were however usually quenched deeply below  $T_g$  and they never recrystallized upon heating. Therefore, it remains to be explored in the future whether the thermal history can affect the level of VDOS in a supercooled liquid close to  $T_g$  and whether crystallization of a sample can cause a systematic offset in the measurement of the melt.

Using the power law approach (eq 1), the terahertz spectra of amorphous, supercooled liquid, and liquid phases can be analyzed in more detail. The fit for paracetamol at several temperatures is shown in Figure 8. Here, the lower cutoff frequency for the fit was fixed to  $\nu_0 = 0.1$  THz, which is the low-frequency limit of our spectrometer.<sup>35</sup>

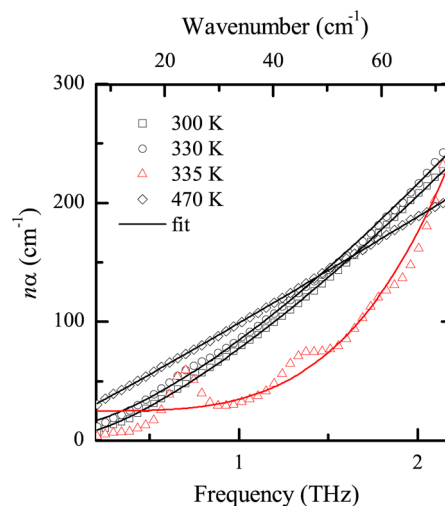


**Figure 8.** Fit by eq 1 of real part of conductivity ( $n\alpha$ ) of supercooled liquid (300 and 330 K), crystalline solid (335 K), and melt (470 K) of paracetamol. It is obvious that the fit is not suitable to describe the spectral features of the crystalline phase.

The fitting parameters  $A$ ,  $C$ , and  $q$  are plotted against temperatures in Figure 9. Parameter  $A$  describes an estimation of losses at frequency  $\nu = \nu_0$ . It is expected to be close to zero in the glassy state and to increase above  $T_g$  as a result of contributions from the dielectric relaxations that shift into the spectral range at higher temperatures.<sup>35</sup> Parameter  $C$  represents the strength of the coupling of terahertz radiation into the sample. In the glassy state, this describes coupling to the VDOS.<sup>30,35</sup> Parameter  $q$  may be used to differentiate between the glassy and liquid states. In the glassy state,  $q$  is expected to be close to 2.<sup>35,40</sup> On the other hand, in the liquid phase,  $q$  is close to 1 as a result of the absorption being dominated by dielectric relaxations. Generally speaking, with the increasing contribution of the dielectric relaxations,  $C$  will increase and  $q$

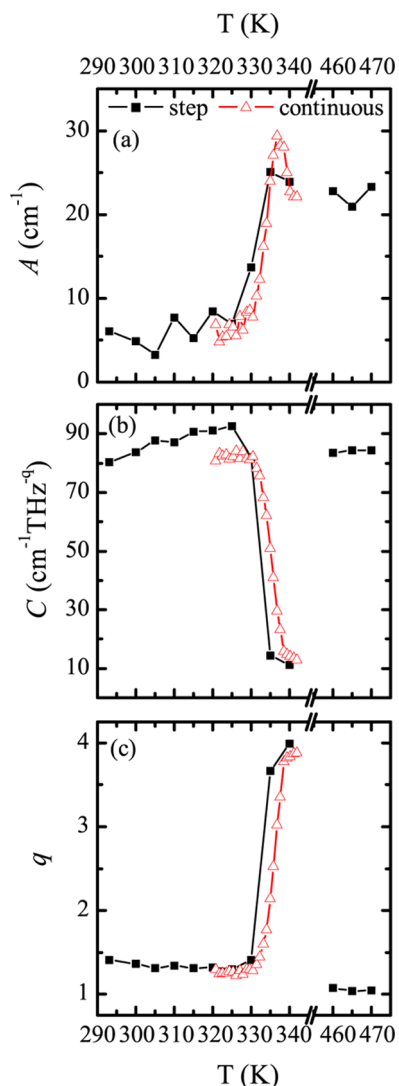


**Figure 9.** Parameters  $A$ ,  $C$  and  $q$  as extracted from the fit of  $n\alpha$  to the experimental spectra using eq 1. The fit was performed on two independently acquired data sets that were obtained by either increasing the temperature step-by-step (black squares) or continuously using a constant ramp rate (red triangles). No values are shown for the temperature range 345–455 K as the sample was crystalline at these temperatures and eq 1 does not apply for crystalline materials. The value of  $A$  obtained from continuous measurement has been offset by  $20\text{ cm}^{-1}$ .

will decrease, which corresponds to the “straightening” of the terahertz spectra that is observed.

**Onset of Crystallization.** From the spectra plotted in Figure 8 it is obvious that the model expressed by eq 1 is not suitable to describe spectra of crystalline samples. In a polycrystalline sample, where the shape of the baseline is strongly linked to scattering of terahertz radiation,<sup>46</sup> it is far from linear and usually well described by a quadratic dependence on frequency.<sup>47</sup> Therefore, the spectra become less “straight” at the onset of crystallization. This deviation from the model can be exploited in order to accurately determine the onset of crystallization, not from a structural perspective as would be resolved by techniques such as X-ray diffraction, but from a molecular dynamics point of view.

In order to do this, we have analyzed the spectra obtained from the continuous measurement at constant temperature

ramp between 320 and 345 K (Figure 5) using the power law eq 1. The results of the fit are shown by red triangles in Figure 9. All three obtained fitting parameters follow the crystallization process above 330 K. There are a number of interesting observations to highlight in this context. As the sample crystallizes, the coupling of terahertz radiation into the VDOS,  $C$ , decreases. This is due to the fact that crystalline materials are dominated by vibrational modes that are associated with long-range order and hence the VDOS breaks down into these discrete modes. As a result, the “baseline” drops between the frequencies of the vibrational modes, even though it does never fully reduce to absolute zero absorption due to scattering and other losses. On the other hand, the exponent of the power law,  $q$ , increases with crystallinity of the sample. Both effects are the result of the spectral shape changing from an almost straight line upon heating-induced crystallization to exhibiting a stronger curvature. The parameters  $C$  and  $q$  suggest that the crystallization is complete at around 340 K. In contrast, parameter  $A$  shows a rather extraordinary decrease above 335 K. This observation highlights that, although the power law is able to fit the spectra obtained from the amorphous phase well, it may suffer from an unequal bias on different fitting parameters in the case of crystalline materials. We therefore conclude that the change in  $A$  above 335 K is not related to the crystallization but presents an artifact from the fitting process of the now crystalline spectra using an equation derived for the amorphous phase.

From Figure 8, it is apparent that the obtained values of  $C$  and  $q$  generally agree between the step-by-step and continuous temperature experiments. The value of  $A$  obtained from the continuous experiment had to be offset by  $20\text{ cm}^{-1}$  in order to match the value from the step-by-step measurement. The origin of this discrepancy is linked to a difference in the spectra at the lowest terahertz frequencies. The exact reason for this is unclear for the time being, but we believe that it is most likely linked to the subtle differences in thermal history between the two samples.

The crystallization kinetics can be described by various models,<sup>48,49</sup> one of the commonly used being the Avrami–Erofeev crystallization kinetics, which is defined by the equation

$$r_c = 1 - e^{(-kt)^n} \quad (2)$$

where  $r_c$  is the crystalline ratio of the sample,  $k$  is the rate constant,  $t$  is time, and  $n$  the exponent reflecting the mechanism of crystallization. For example, for  $n = 3$ , the model is known also as the “random nucleation and growth” mechanism.<sup>49</sup>

The crystalline ratio  $r_c$  can be also expressed as  $r_c = 1 - r_a$ , where  $r_a$  is the corresponding amorphous ratio. In order to reflect the fact that the crystallization of the amorphous sample does not start immediately with the beginning of the heating experiment, given that we start acquiring at temperatures well below the onset of crystallization, eq 2 can be modified to

$$r_c = 1 - e^{(-k(t-t_0))^n}$$

$$r_a = e^{(-k(t-t_0))^n} \quad (3)$$

Here,  $t_0$  is for the onset time of the crystallization relative to the beginning of the continuous temperature ramp. In order to determine the accurate onset of the crystallization, the fit was performed only on the data with an apparent presence of crystalline phase, that is, for temperatures above 330 K. This is crucial as one of the prerequisites of the Avrami–Erofeev

model is the existence of a nucleus from which the growth of the crystalline phase occurs.

The Avrami–Erofeev crystallization kinetics model can be used to fit the values of  $C$  and  $q$  between 330 and 340 K; however, before eq 2 can be used, the values must be normalized. The normalized values  $C_{\text{norm}}$  and  $q_{\text{norm}}$  were obtained by subtracting the baseline value at the highest temperatures for  $C$  and the lowest temperatures for  $q$  and rescaling the data to 1. Given that  $C$  decreases and  $q$  increases upon crystallization,  $C_{\text{norm}}$  was assigned to  $r_a$  and  $q_{\text{norm}}$  with  $r_c$  in order to perform the Avrami–Erofeev fitting using eqs 3. The rescaled parameters  $C_{\text{norm}}$  and  $q_{\text{norm}}$  are shown in Figure 10a,

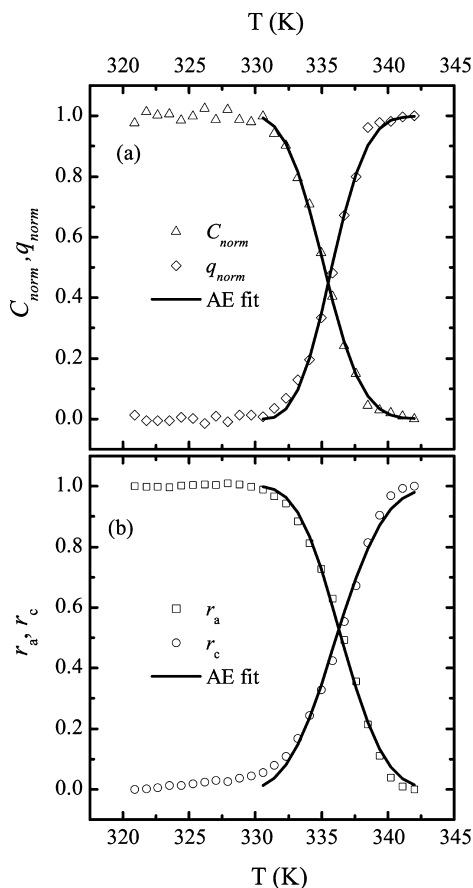


**Figure 10.** Avrami–Erofeev (AE) fit of (a) normalized values of  $C$  and  $q$  obtained from power law fit eq 1 and (b) amorphous and crystalline ratio obtained from fit of spectra by eq 4

together with the fit by the Avrami–Erofeev model where  $n = 3$ . The value of  $n$  was chosen to reflect the fact that crystallization from a covered sample of paracetamol is dominated by bulk crystallization.<sup>9</sup>

A different way to express  $r_a$  and  $r_c$  is by assuming that the absorption spectra  $\alpha(T, \nu)$  of the sample at any given temperature between purely amorphous and purely crystalline form are described by

$$\alpha(T, \nu) = r_a(T)\alpha_a(\nu) + r_c(T)\alpha_c(\nu) \quad (4)$$

where  $T$  is temperature,  $\nu$  is frequency, and  $\alpha_a$  and  $\alpha_c$  are the absorption spectra of the purely amorphous and purely crystalline form. Using this method, the data obtained from the continuous temperature spectroscopy were analyzed (Figure 5), where amorphous spectra  $\alpha_a$  corresponded to the

spectra at 320 K and the crystalline spectra  $\alpha_c$  corresponded to the absorption level at 422 K, that is, at the spectra at lowest and the highest temperature, respectively. The obtained amorphous ( $r_a(T)$ ) and crystalline ( $r_c(T)$ ) ratios are shown in Figure 10b. Similarly to the case of  $C_{\text{norm}}$  and  $q_{\text{norm}}$ , the values of  $r_a$  and  $r_c$  have been fitted using the Avrami–Erofeev model eqs 3 with  $n = 3$  reflecting the bulk crystallization of paracetamol.<sup>9</sup>

The obtained values for the crystallization rate  $k$  and onset of crystallization  $t_0$  are summarized in Table 1. The values are

**Table 1.** Values of Crystallization Rate  $k$  and Onset Time of Crystallization  $t_0$  (Converted to the Corresponding Temperature  $T$ ) Obtained Using the Avrami–Erofeev Fits of  $C_{\text{norm}}$ ,  $q_{\text{norm}}$ ,  $r_c$ , and  $r_a$  As Defined in Equation 4<sup>a</sup>

	$k/\text{min}^{-1}$	$t_0/\text{min}$
$C_{\text{norm}}$	0.059	23.1 ( $T = 329.2$ K)
$q_{\text{norm}}$	0.065	25.9 ( $T = 330.4$ K)
$r_c$	0.047	21.5 ( $T = 328.6$ K)
$r_a$	0.053	24.5 ( $T = 329.8$ K)
DSC (tangent method)		$T = 332$ K
DSC (onset of deviation)		$T = 328$ K

<sup>a</sup>The last two lines represent the onset of crystallisation obtained from DSC as shown in Figure 11.

similar, although  $C_{\text{norm}}$  and  $q_{\text{norm}}$  result in slightly higher crystallization rate  $k$  and later onset of crystallization  $t_0$  than the values obtained from the fit of  $r_c$  and  $r_a$ . The values of  $C_{\text{norm}}$  and  $q_{\text{norm}}$  are however more vulnerable toward errors given the fact that the power law is not a very good fit for the terahertz spectra of semicrystalline samples and it needed to be normalized. The onset temperature of crystallization matches well with the temperature measured by DSC. The DSC value determined using the tangents method (Figure 11) is slightly

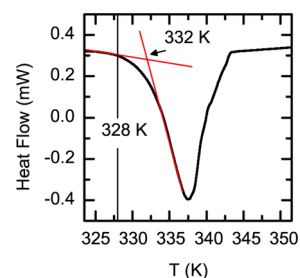


**Figure 11.** DSC of the crystallization of amorphous paracetamol at a heating rate of  $0.4 \text{ K min}^{-1}$  (endotherms pointing down). The red solid lines represent the tangents used to determine the onset of crystallization at 332 K. The vertical line at 328 K highlights the onset temperature where the heat flow deviates from the baseline tangent.

higher than the values obtained using the Avrami–Erofeev fits. The fitted values are much closer to the onset of deviation of the heat flow from its baseline tangent, which seems intuitive as our terahertz method detects subtle changes in the intermolecular arrangement.

The idea of splitting the spectra into crystalline and amorphous fractions using eq 4 has also its limitations. The sum  $r_a + r_c$  is expected to be unity at all temperatures and times. In order to meet this criterion, only spectra up to 1.2 THz were used, and overall, it can be stated that  $1 < r_a + r_c < 1.06$ . When a broader spectral range is used, the sum will be generally higher,

but narrowing the range further had no effect on the sum. One of the reasons for the sum exceeding unity is likely to originate from additional scattering from some crystalline or amorphous parts of the sample as the grain structure of the sample changes during crystallization. Another reason is the slight increase in absorption level of the amorphous part of the sample with increasing temperature given the non-isothermal conditions. Although, overall, the model works well in our case, it may be even more suitable for an isothermal study of a crystallization process.

## CONCLUSIONS

The crystallization and subsequent melting has been studied for a sample of amorphous paracetamol at terahertz frequencies. Upon heating amorphous paracetamol, crystallization into form III is observed, followed by phase transitions to forms II and I at higher temperatures. This observation is in agreement with a previous study of paracetamol by low-frequency Raman scattering,<sup>9</sup> where the authors observed the same sequence of polymorphic forms appearing under similar sample conditions (sample covered and here additionally under vacuum). The featureless spectra that are observed at terahertz frequencies for the supercooled liquid and liquid melt can both be fitted using a modified power law model. The main difference between the terahertz absorption of the liquid melt and the supercooled liquid is that the melt spectrum is dominated by the dielectric relaxation as well as the VDOS, while in the supercooled liquid the contribution due to the dielectric relaxation vanishes close to  $T_g$ , which is reflected by a change of the power law exponent from 2 in the glassy state to 1 in the liquid melt state. We demonstrate that the spectral deviation from the power law model can be used as a very sensitive probe for the onset of crystallization. In addition, we have revealed evidence that the crystallization has a stronger effect on the vibrational characteristics of the materials when compared to the dielectric relaxation properties. Using the terahertz spectra together with a power law fit, we were able to demonstrate a method of extracting quantitative kinetic information from the spectra based on the Avrami–Erofeev mechanism. We determined an effective rate constant of  $k = 0.056 \text{ min}^{-1}$  with a corresponding onset of crystallization at  $T = 329.5 \text{ K}$  for a heating rate of  $0.4 \text{ K min}^{-1}$ . The method described in this work is applicable to investigate crystallization event of any hydrogen-bonded organic molecular crystals.

## AUTHOR INFORMATION

### Corresponding Author

\*E-mail: jaz22@cam.ac.uk

### Notes

The authors declare no competing financial interest.

## ACKNOWLEDGMENTS

J.S. would like to thank the UK Engineering and Physical Sciences Research Council (EPSRC) for financial support. The authors would like to thank the support by the Department of Chemical Engineering and Biotechnology for M.J.S. and M.F., who undertook this work as part of their final year undergraduate research project.

## REFERENCES

(1) Hancock, B. C.; Parks, M. What is the true solubility advantage for amorphous pharmaceuticals? *Pharm. Res.* **2000**, *17*, 397–404.

(2) Laitinen, R.; Löbmann, K.; Strachan, C. J.; Grohgan, H.; Rades, T. Emerging trends in the stabilization of amorphous drugs. *Int. J. Pharm.* **2013**, *453*, 65–79.

(3) Bhattacharya, S.; Suryanarayanan, R. Local mobility in amorphous pharmaceuticals: characterization and implications on stability. *J. Pharm. Sci.* **2009**, *98*, 2935–2953.

(4) Perlovich, G. L.; Volkova, T. V.; Bauer-Brandl, A. Polymorphism of paracetamol. Relative stability of the monoclinic and orthorhombic phase revisited by sublimation and solution calorimetry. *J. Therm. Anal. Calorim.* **2007**, *89*, 767–774.

(5) Di Martino, P.; Palmieri, G. F.; Martelli, S. Molecular mobility of the paracetamol amorphous form. *Chem. Pharm. Bull.* **2000**, *48*, 1105–1108.

(6) Johari, G. P.; Kim, S.; Shanker, R. M. Dielectric studies of molecular motions in amorphous solid and ultraviscous acetaminophen. *J. Pharm. Sci.* **2005**, *94*, 2207–2023.

(7) Di Martino, P.; Conflant, P.; Drache, M.; Huvenne, J. P.; Guyot-Hermann, A. M. Preparation and physical characterization of forms II and III of paracetamol. *J. Therm. Anal.* **1997**, *48*, 447–458.

(8) Qi, S.; Avalle, P.; Saklatvala, R.; Craig, D. Q. M. An investigation into the effects of thermal history on the crystallisation behaviour of amorphous paracetamol. *Eur. J. Pharm. Biopharm.* **2008**, *69*, 364–371.

(9) Nanubolu, J. B.; Burley, J. C. Investigating the recrystallization behavior of amorphous paracetamol by variable temperature Raman studies and surface Raman mapping. *Mol. Pharmaceutics* **2012**, *9*, 1544–1558.

(10) Baird, J. A.; Taylor, L. S. Evaluation of amorphous solid dispersion properties using thermal analysis techniques. *Adv. Drug Delivery Rev.* **2012**, *64*, 396–421.

(11) Correia, N. T.; Ramos, J. J.; Descamps, M.; Collins, G. Molecular mobility and fragility in indomethacin: a thermally stimulated depolarization current study. *Pharm. Res.* **2001**, *18*, 1767–1774.

(12) Guo, Y.; Shalae, E.; Smith, S. Physical stability of pharmaceutical formulations: solid-state characterization of amorphous dispersions. *Trends Anal. Chem.* **2013**, *49*, 137–144.

(13) Shamblin, S. L.; Tang, X.; Chang, L.; Hancock, B. C.; Pikal, M. J. Characterization of the time scales of molecular motion in pharmaceutically important glasses. *J. Phys. Chem. B* **1999**, *103*, 4113–4121.

(14) Van den Mooter, G.; Augustijns, P.; Kinget, R. Stability prediction of amorphous benzodiazepines by calculation of the mean relaxation time constant using the Williams-Watts decay function. *Eur. J. Pharm. Biopharm.* **1999**, *48*, 43–48.

(15) Johari, G. P.; Kim, S.; Shanker, R. M. Dielectric relaxation and crystallization of ultraviscous melt and glassy states of aspirin, ibuprofen, progesterone, and quinidine. *J. Pharm. Sci.* **2007**, *96*, 1159–1175.

(16) Grzybowska, K.; Paluch, M.; Grzybowski, A.; Wojnarowska, Z.; Hawelek, L.; Kolodziejczyk, K.; Ngai, K. L. Molecular dynamics and physical stability of amorphous anti-inflammatory drug: celecoxib. *J. Phys. Chem. B* **2010**, *114*, 12792–12801.

(17) Johari, G.; Shanker, R. M. On determining the relaxation time of glass and amorphous pharmaceuticals stability from thermodynamic data. *Thermochim. Acta* **2010**, *511*, 89–95.

(18) Cicerone, M. T.; Soles, C. L. Fast dynamics and stabilization of proteins: binary glasses of trehalose and glycerol. *Biophys. J.* **2004**, *86*, 3836–3845.

(19) Cicerone, M. T.; Douglas, J. F.  $\beta$ -Relaxation governs protein stability in sugar-glass matrices. *Soft Matter* **2012**, *8*, 2983.

(20) Taday, P. F. Applications of terahertz spectroscopy to pharmaceutical sciences. *Philos. Trans. R. Soc. London, Ser. A* **2004**, *362*, 351–363.

(21) Zeitler, J. A.; Taday, P. F.; Newnham, D. A.; Pepper, M.; Gordon, K. C.; Rades, T. Terahertz pulsed spectroscopy and imaging in the pharmaceutical setting: a review. *J. Pharm. Pharmacol.* **2007**, *59*, 209–223.



- (22) Jepsen, P.; Cooke, D.; Koch, M. Terahertz spectroscopy and imaging: modern techniques and applications. *Laser Photonics Rev.* **2011**, *124*–166.
- (23) Strachan, C. J.; Taday, P. F.; Newnham, D. A.; Gordon, K. C.; Zeitler, J. A.; Pepper, M.; Rades, T. Using terahertz pulsed spectroscopy to quantify pharmaceutical polymorphism and crystallinity. *J. Pharm. Sci.* **2005**, *94*, 837–846.
- (24) Zeitler, J. A.; Newnham, D. A.; Taday, P. F.; Threlfall, T. L.; Lancaster, R. W.; Berg, R. W.; Strachan, C. J.; Pepper, M.; Gordon, K. C.; Rades, T. Characterization of temperature-induced phase transitions in five polymorphic forms of sulfathiazole by terahertz pulsed spectroscopy and differential scanning calorimetry. *J. Pharm. Sci.* **2006**, *95*, 2486–2498.
- (25) Zeitler, J. A.; Kogermann, K.; Rantanen, J.; Rades, T.; Taday, P. F.; Pepper, M.; Aaltonen, J.; Strachan, C. J. Drug hydrate systems and dehydration processes studied by terahertz pulsed spectroscopy. *Int. J. Pharm.* **2007**, *334*, 78–84.
- (26) Nguyen, K. L.; Frisci , T.; Day, G. M.; Gladden, L. F.; Jones, W. Terahertz time-domain spectroscopy and the quantitative monitoring of mechanochemical cocrystal formation. *Nat. Mater.* **2007**, *6*, 206–209.
- (27) Parrott, E. P. J.; Zeitler, J. A.; Frisci , T.; Pepper, M.; Jones, W.; Day, G. M.; Gladden, L. F. Testing the sensitivity of terahertz spectroscopy to changes in molecular and supramolecular structure: a study of structurally similar cocrystals. *Cryst. Growth Des.* **2009**, *9*, 1452–1460.
- (28) Grischkowsky, D.; Keiding, S.; Exter, M. V.; Fattinger, C. Far-infrared time-domain spectroscopy with terahertz beams of dielectrics and semiconductors. *J. Opt. Soc. Am. B* **1990**, *7*, 2006.
- (29) Naftaly, M.; Miles, R. Terahertz time-domain spectroscopy: a new tool for the study of glasses in the far infrared. *J. Non-Cryst. Solids* **2005**, *351*, 3341–3346.
- (30) Taraskin, S.; Sindyankin, S.; Elliott, S.; Neilson, J.; Lo, T. Universal features of terahertz absorption in disordered materials. *Phys. Rev. Lett.* **2006**, *97*, 055504.
- (31) Parrott, E. P. J.; Zeitler, J. A.; Simon, G.; Hehlen, B.; Gladden, L. F.; Taraskin, S. N.; Elliott, S. Atomic charge distribution in sodosilicate glasses from terahertz time-domain spectroscopy. *Phys. Rev. B* **2010**, *82*, 140203.
- (32) Zalkovskij, M.; Bisgaard, C. Z.; Novitsky, A.; Malureanu, R.; Savastru, D.; Popescu, A.; Jepsen, P. U.; Lavrinenko, A. V. Ultrabroadband terahertz spectroscopy of chalcogenide glasses. *Appl. Phys. Lett.* **2012**, *100*, 031901.
- (33) Wietzke, S.; Jansen, C.; Jung, T.; Reuter, M.; Baudrit, B.; Bastian, M.; Chatterjee, S.; Koch, M. Terahertz time-domain spectroscopy as a tool to monitor the glass transition in polymers. *Opt. Express* **2009**, *17*, 19006–19014.
- (34) Wietzke, S.; Jansen, C.; Reuter, M.; Jung, T.; Kraft, D.; Chatterjee, S.; Fischer, B. M.; Koch, M. Terahertz spectroscopy on polymers: a review of morphological studies. *J. Mol. Struct.* **2011**, *1006*, 41–51.
- (35) Sibik, J.; Shalaev, E. Y.; Zeitler, J. A. Glassy dynamics of sorbitol solutions at terahertz frequencies. *Phys. Chem. Chem. Phys.* **2013**, *15*, 11931–11942.
- (36) Sibik, J.; Elliott, S. R.; Zeitler, J. A. Thermal decoupling of molecular relaxation processes from the vibrational density of states at terahertz frequencies in supercooled hydrogen-bonded liquids. Submitted for publication.
- (37) Zeitler, J. A.; Taday, P. F.; Pepper, M.; Rades, T. Relaxation and crystallization of amorphous carbamazepine studied by terahertz pulsed spectroscopy. *J. Pharm. Sci.* **2007**, *96*, 2703–2709.
- (38) Hoshina, H.; Ishii, S.; Yamamoto, S.; Morisawa, Y.; Sato, H.; Uchiyama, T.; Ozaki, Y.; Otani, C. Terahertz spectroscopy in polymer research: assignment of intermolecular vibrational modes and structural characterization of poly(3-hydroxybutyrate). *IEEE Trans. Terahertz Sci. Technol.* **2013**, 248–258.
- (39) Parrott, E. P. J.; Zeitler, J. A.; McGregor, J.; Oei, S.-P.; Unalan, H. E.; Tan, S.-C.; Milne, W. I.; Tessonnier, J.-P.; Schl gl, R.; Gladden, L. F. Understanding the dielectric properties of heat-treated carbon nanofibers at terahertz frequencies: a new perspective on the catalytic activity of structured carbonaceous materials. *J. Phys. Chem. C* **2009**, *113*, 10554–10559.
- (40) Strom, U.; Hendrickson, J. R.; Wagner, R. I.; Taylor, P. C. Disorder-induced far infrared absorption in amorphous materials. *Solid State Commun.* **1974**, *15*, 1871–1875.
- (41) Delaney, S. P.; Pan, D.; Yin, S. X.; Smith, T. M.; Korter, T. M. Evaluating the roles of conformational strain and cohesive binding in crystalline polymorphs of aripiprazole. *Cryst. Growth Des.* **2013**, *13*, 2943–2952.
- (42) Burnett, A. D.; Kendrick, J.; Russell, C.; Christensen, J.; Cunningham, J. E.; Pearson, A. R.; Linfield, E. H.; Davies, A. G. Effect of molecular size and particle shape on the terahertz absorption of a homologous series of tetraalkylammonium salts. *Anal. Chem.* **2013**, *85*, 7926–7934.
- (43) Singh, R.; George, D. K.; Benedict, J. B.; Korter, T. M.; Markelz, A. G. Improved mode assignment for molecular crystals through anisotropic terahertz spectroscopy. *J. Phys. Chem. A* **2012**, *116*, 10359–10364.
- (44) Zeitler, J. A.; Newnham, D. A.; Taday, P. F.; Strachan, C. J.; Pepper, M.; Gordon, K. C.; Rades, T. Temperature dependent terahertz pulsed spectroscopy of carbamazepine. *Thermochim. Acta* **2005**, *436*, 71–77.
- (45) Yannopoulos, S.; Andrikopoulos, K.; Ruocco, G. On the analysis of the vibrational Boson peak and low-energy excitations in glasses. *J. Non-Cryst. Solids* **2006**, *352*, 4541–4551.
- (46) Melinger, J.; Laman, N.; Harsha, S.; Grischkowsky, D. Line narrowing of terahertz vibrational modes for organic thin polycrystalline films within a parallel plate waveguide. *Appl. Phys. Lett.* **2006**, *89*, 251110.
- (47) Shen, Y.; Taday, P. F.; Pepper, M. Elimination of scattering effects in spectral measurement of granulated materials using terahertz pulsed spectroscopy. *Appl. Phys. Lett.* **2008**, *92*, 051103.
- (48) Seefeldt, K.; Miller, J.; Alvarez-Nunez, F.; Rodriguez-Hornedo, N. Crystallization pathways and kinetics of Carbamazepine–nicotinamide cocrystals from the amorphous state by in situ thermomicroscopy, spectroscopy and calorimetry studies. *J. Pharm. Sci.* **2007**, *96*, 1147–1158.
- (49) Li, H.; Stowell, J. G.; He, X.; Morris, K. R.; Byrn, S. R. Investigations on solid–solid phase transformation 5-methyl-2-[(4-methyl-2-nitrophenyl)amino]-3- thiophenecarbonitrile. *J. Pharm. Sci.* **2007**, *96*, 1079–1089.